Molecular Crystals and Liquid Crystals

ISSN: 1542-1406 (Print) 1563-5287 (Online) Journal homepage: https://www.tandfonline.com/loi/gmcl20

Synthesis and Mesogenic Properties of Liquid Crystals Based on Cholesterol and Cinnamic Acid Derivatives

Xuenan Zong & Changcheng Wu

To cite this article: Xuenan Zong & Changcheng Wu (2018) Synthesis and Mesogenic Properties of Liquid Crystals Based on Cholesterol and Cinnamic Acid Derivatives, Molecular Crystals and Liquid Crystals, 666:1, 40-53, DOI: 10.1080/10691316.2018.1541843

To link to this article: https://doi.org/10.1080/10691316.2018.1541843

Published online: 27 Feb 2019.

MOLECULAR CRYSTALS AND LIQUID CRYSTALS
2018, VOL. 666, NO. 1, 60–73
https://doi.org/10.1080/10691316.2018.1541843

Synthesis and Mesogenic Properties of Liquid Crystals Based on Cholesterol and Cinnamic Acid Derivatives

Xuenan Zong and Changcheng Wu

School of Material Science & Engineering, Tianjin Polytechnic University, Tianjin 300387, PR, China

ABSTRACT

A group of new mesomorphic compounds with cholesterol-based, which have derivative of the cinnamic acid, with different lengths of terminal alkoxy chains, are synthesized and characterized. The mesomorphic properties were investigated by DSC and POM. All target compounds showed a cholesteric phase. For 12-TC and 14-TC besides a cholesteric phase, also revealed a SmA* phase. The experimental results demonstrated that with the increase in the terminal chain lengths, the thermal stability of the smectic mesophases of these liquid crystals was increased, and these compounds shows brilliant color changes in the temperature ranges of cholesteric phase.

KEYWORDS

Liquid crystal; cholesterol-based; cinnamic acid; terminal alkoxy chain; synthesis

1. Introduction

Because of its unique thermoelectric properties, liquid crystal compounds have been widely used in many fields, such as photoelectric materials, information storage and biomedicine [1–11]. The double bonds of cinnamic acid been attracting attention in the field of liquid crystal due to bond isomerization, and thus to switching the mesomorphic properties, and to photodimerisation and cross-linking the molecules in the liquid crystalline state [12]. The presence of double bonds in cinnamic acid results in the formation of rod-like molecules and enhances the thermal stability of the mesophase, which has attracted research interest in the domain of liquid crystals [13–16]. In recent years, cholesterol-based dimers have received extensive attention and research. This can be attributed to their unique molecular structural features that not only result in a stable mesophase, but also produce a variety of liquid crystal texture. In particular, their phase behavior seems to depend heavily on the length of the flexible chain [17–20]. The length of the alkyl chain has a considerable influence on many properties such as phase transition temperature, phase structure, dielectric anisotropy, and optical anisotropy. For these reasons, different liquid crystal properties can be obtained through the change in spacer length and terminal chain length [21–32]. By changing the position and length of the alkyl chain, the same series of liquid crystal compounds can exhibit different liquid crystal mesophases such as nematic, Col_h, smectic A* and C phases [33–44]. In this article, we report on the synthesis and the mesomorphic properties of a new series of the cinnamic acid and cholesteryl derivatives that have at one side a

CONTACT Changcheng Wu ccwu@tjpu.edu.cn School of Material Science & Engineering, Tianjin Polytechnic University, Tianjin, 300160, China.

different number of alkyl chains with a different number of carbon atoms and, at the other side, a cholesterol-based. This study indicated that the dependence of mesomorphism (mesophase type, stability and thermal range) and thermo-optical features on the length of their terminal chain.

The molecular structures of the target compounds were characterized by elemental analysis, Fourier transforms infrared spectroscopy (FT-IR) and ^{1}H NMR techniques. Their liquid crystal properties were investigated by differential scanning calorimetry (DSC) and polarizing optical microscopy (POM).

2. Experimental

2.1. Material

All the chemicals and solvents were obtained from commercial sources. The crude samples were purified by column chromatography using silica gel (400 mesh). 1-bromobutane, 1-bromohexane, 1-bromooctane, 1-bromodecane, 1-bromododecane, 1-Bromotetradecane, anhydrous EtOH, 4-Benzyloxyphenol, Methanol and ptoluenesulfonic acid (PTSA) were GR grade reagents, Cholesterol succinic acid monoester was prepared from our previous work [32]. Dichloromethane (DCM) and tetrahydrofuran (THF) were dried over CaH_2. All other solvents and reagents were purchased commercially and used without any further purification.

2.2. Characterization

Chemical structures of the intermediates and dimesogenic compounds were characterized with FT-IR by using Bruker Tensor 307 spectrometer and ^{1}H NMR spectrum by using Bruker 400MHz with tetramethylsilane as an internal standard. Compositions of the compounds were determined by vario El cube Elemental analyzer. The phase transitions of the dimesogenic compounds were determined by means of the Olympus BX51 polarized optical microscope (POM) equipped with Linkam THMS600 hot stage. A differential scanning calorimeter (DSC) (Netzsch DSC204) was used to measure the transformation temperature and transformation enthalpy at the heating rate of 10°C/min.

2.3. Synthesis

The synthetic route used in the preparation of target compounds series as seen in Scheme 1, it involved three steps: (1) Synthesis of methyl p-hydroxycinnamate from p-hydroxycinnamic acid and subsequent reaction with different bromoalkyl groups to obtain p-alkoxycinnamate (m-A) and further reaction to produce p-alkoxycinnamic acid (m-B) (2) Cholesterol succinic acid monoester reacts with 4-benzyloxyphenol to form ester (C), which is then dehydrogenated to phenol (D) (3) Esterification of alkoxycinnamic acids (B) and D produces the final product m-TC (Where m is the number of carbon atoms in the terminal alkyl chain, m = 4, 6, 8, 10, 12 and 14). The synthetic route used to prepare this series of target compounds is shown in Scheme 1.

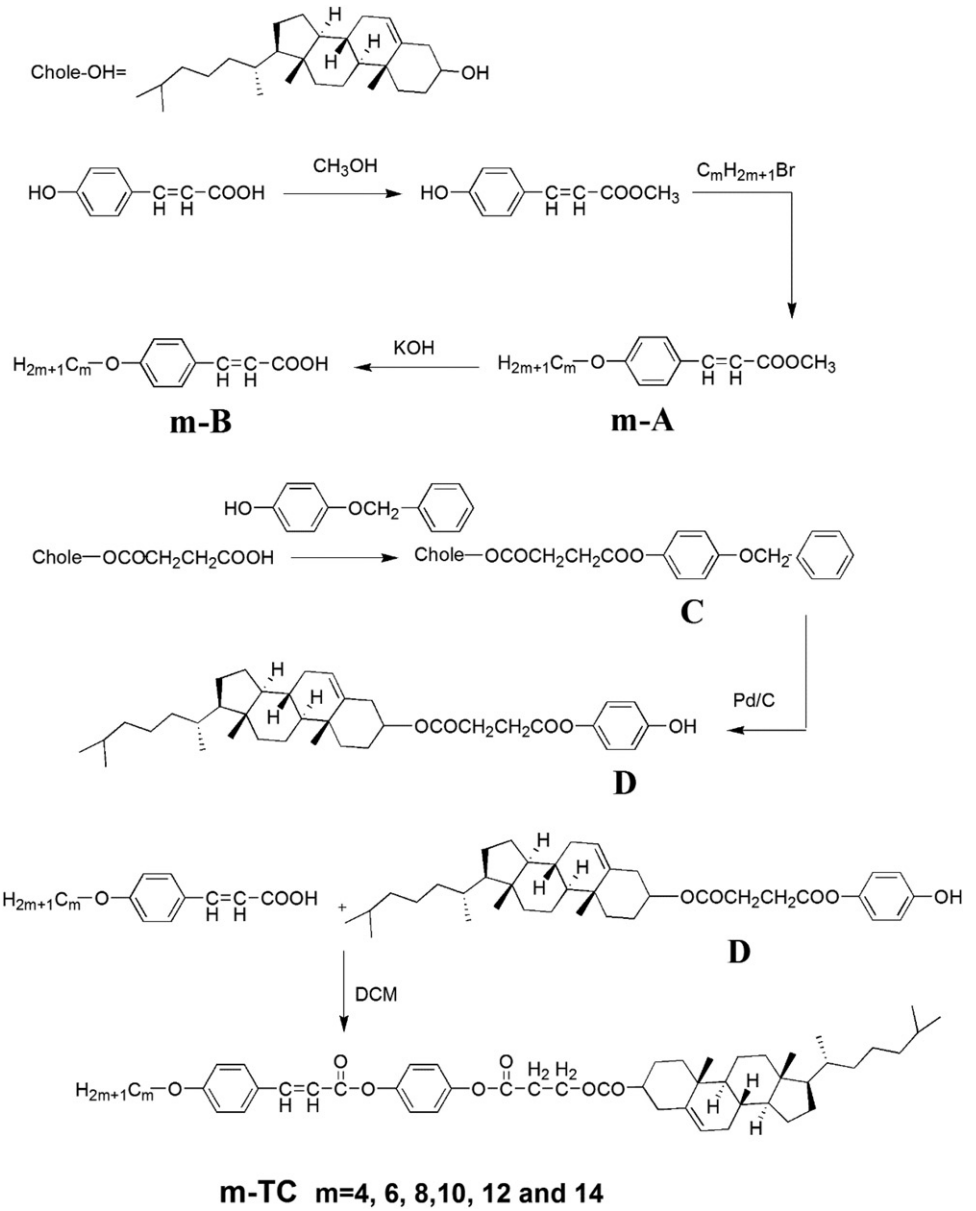

Scheme 1. The synthesis route of the final product m-TC (where m is the number of carbon atoms in the terminal alkyl chain)

2.3.1. Methyl p-hydroxycinnamate

16 mmol (2.64 g) of p-hydroxycinnamic acid, 0.25 g of p-toluenesulfonic acid, dissolved in 40 ml of anhydrous methanol, and heated under reflux for 8 hours. It was synthesized following the similar method described in the literature [45]. It was purified by column chromatography with silica gel using petroleum ether/ethyl acetate = 6:1. The resulting product was white solid. Yield: 82%。

2.3.2. Methyl p-alkoxycinnamate (m-B)

3 mmol (0.543 g) of methyl p-hydroxycinnamate and 6 mmol (0.83 g) of K_2CO_3, 0.2 g of KI were dissolved in 30 ml of butanone, 3.6 mmol (0.493 g) 1-bromobutane was dripped into the vigorously stirring solution. After the reaction, the crude was washed with water and then filtrated and dried under vacuum to afford the product as a white solid (4-A). Yield: 79.3%. 3mmol 4-A and 9mmol KOH 0.504 g were dissolved in 10ml of water, and heated to reflux for 4 hours. After completing the reaction, 100ml water was added, neutralize to pH =3-4 with concentrated hydrochloric acid. The crude was washed with water, then filtrated and dried under vacuum to afford product as a white solid (4-B). Yield: 72.5%。 ^{1}HNMR ($CDCl_3$, 400M, ppm): δ 7.74 (d, 1H), 7.50 (d, 2H), 6.91 (d, 2H), 6.31 (d, 1H), 4.00 (t, 2H), 1.83-0.98 (m, 7H). FTIR (KBr, cm^{-1}): 2938, 2868, 1666, 1596, 1510, 1432, 1170, 944, 822, 517.

Reactions with 1-bromohexane, 1-bromooctane, 1-bromodecane, 1-bromododecane and 1-bromotetradecane to form m-B (m = 6, 8, 10, 12 and 14), respectively, and the synthesis method remains unchanged.

6-B: ^{1}HNMR ($CDCl_3$, 400M, ppm): δ 7.74 (d, 1H), 7.50 (d, 2H), 6.91 (d, 2H), 6.31 (d, 1H), 3.99 (t, 2H), 1.84-0.87 (m, 11H). FTIR (KBr, cm^{-1}): 2938, 2868, 1666, 1596, 1510, 1432, 1300, 1214, 1170, 979, 822, 578, 517.

8-B: ^{1}HNMR ($CDCl_3$, 400M, ppm): δ 7.73 (d, 1H), 7.49 (d, 2H), 7.02 (m, 2H), 6.31 (d, 1H), 3.95 (dt, 2H), 1.92-0.89 (m, 15H). FTIR (KBr, cm^{-1}): 2920, 2850, 1666, 1596, 1510, 1432, 1300, 1240, 1222, 1170, 979, 831, 726, 587, 517.

10-B: ^{1}HNMR ($CDCl_3$, 400M, ppm): δ 7.74 (d, 1H), 7.49 (d, 2H), 6.91 (d, 2H), 6.31 (d, 1H), 3.99 (t, 2H), 1.84-0.88(m, 19H). FTIR (KBr, cm^{-1}): 2920, 2850, 1666, 1596, 1510, 1432, 1300, 1240, 1170, 979, 822, 717, 578, 517.

12-B: ^{1}HNMR ($CDCl_3$, 400M, ppm): δ 7.73 (d, 1H), 7.49 (d, 2H), 6.91 (d, 2H), 6.31 (d, 1H), 3.99 (t, 2H), 1.79-0.88 (m, 23H). FTIR (KBr, cm^{-1}): 2920, 2850, 1666, 1596, 1510, 1432, 1309, 1240, 1214, 1170, 979, 822, 717, 587, 517.

14-B: ^{1}HNMR ($CDCl_3$, 400M, ppm): δ 7.72 (d, 1H), 7.49 (d, 2H), 6.90 (d, 2H), 6.31 (d, 1H), 3.99 (t, 2H), 1.83-0.88(m, 27H). FTIR (KBr, cm^{-1}): 2920, 2850, 1666, 1596, 1510, 1432, 1300, 1240, 1170, 979, 831, 717, 517.

2.3.3. Cholesterol 4-hydroxy-4′-ethoxy carbonate

Cholesterol succinic acid monoester 5mmol (2.43g), 4-benzyloxyphenol 5mmol (1g) and DMAP 1mmol (1g) were dissolved in anhydrous CH_2Cl_2 (30 mL), DCC 6mmol (1.236g) was dissolved in 10mL of CH_2Cl_2 and dripped into the vigorously stirring solution. After completing the reaction, the resulting solution was washed with distilled water twice and drying over $MgSO_4$. The product was purified by silica gel column chromatography using petroleum ether/ethyl acetate 6:1 as the eluent. Then, palladium carbon, which is one-tenth of the weight of the reactants, was added and reacted under a hydrogen atmosphere for 6 hours in THF solution. After the reaction was stopped, it was filtered and recrystallized from petroleum ether/ethyl acetate. Yield:49.8%。 ^{1}H NMR ($CDCl_3$, 400M, ppm): δ 6.95 (d, 2H), 6.84-6.76 (m, 2H), 5.37 (d, 1H), 4.65 (d, 1H), 2.85 (t, 2H), 2.71 (t, 2H), 2.33-0.83 (m, 44H). FTIR (KBr, cm^{-1}): 3416, 2859, 1719, 1510, 1187, 1127, 995, 840, 796, 517.

2.3.4 The target compounds (m-TC)

(4-B) 0.5mmol (0.289g), Cholesterol 4-hydroxy-4'-ethoxy carbonate 0.5mmol (0.11g) and DMAP 1mmol (1g) were dissolved in anhydrous CH_2Cl_2 (30 mL), DCC 0.525mmol (0.108g) was dissolved in 10mL of CH_2Cl_2 and dripped into the vigorously stirring solution. The reaction mixture was stirred for 24 h at room temperature. After completing the reaction, the resulting solution was washed with distilled water twice and drying over $MgSO_4$. The product was purified by silica gel column chromatography using petroleum ether/ethyl acetate 6:1 as the eluent. Yield:54.3%。^{1}H NMR ($CDCl_3$, 400M, ppm): δ 7.81 (d, 1H), 7.52-6.92 (m, 8H), 6.47 (d, 1H), 5.38 (m, 1H), 4.57 (m, 1H), 4.01 (t, 2H), 2.88-0.68 (t, 54H). FTIR (KBr, cm^{-1}): 520, 824, 1129, 1175, 1259, 1499, 1600, 1730, 2867, 2931. Elemental analysis: Calculated: C 76.89%, H 8.78%. Found: C 76.66%, H 8.92%.

Five compounds 6-TC, 8-TC, 10-TC, 12-TC and 14-TC were prepared by the same method. In the above, the synthesis of 4-TC will be described as an example.

6-TC: ^{1}H NMR ($CDCl_3$, 400M, ppm): δ 7.81 (d, 1H), 7.52-6.92 (m, 8H), 6.47 (d, 1H), 5.38 (d, 1H), 4.65 (s, 1H), 4.00 (t, 2H), 2.80- 0.68 (m, 58H). FTIR (KBr, cm^{-1}): 520, 824, 1120, 1175, 1250, 1499, 1600, 1730, 2867, 2931. Elemental analysis: Calculated: C 77.19%, H 8.97%. Found: C 77.29%, H 9.29%.

8-TC: ^{1}H NMR ($CDCl_3$, 400M, ppm): δ 7.81 (d, 1H), 7.57-6.85 (m, 8H), 6.51 (d, 1H), 5.38 (d, 1H), 4.68(s, 1H), 4.00 (t, 2H), 2.81-0.65 (m, 62H). FTIR (KBr, cm^{-1}): 520, 822, 1127, 1500, 1510, 1605, 1728, 2857, 2931. Elemental analysis: Calculated: C 77.47%, H 9.15%. Found: C 77.95%, H 9.35%.

10-TC: ^{1}H NMR ($CDCl_3$, 400M, ppm): δ 7.81 (d, 1H), 7.58-6.85 (m, 8H), 6.48 (d, 1H),5.38 (d, 1H), 4.67(s, 1H), 4.00 (t, 2H), 2.87-0.68 (m, 66H). FTIR (KBr, cm^{-1}): 520, 824, 1120, 1175, 1250, 1472, 1500, 1600, 1730, 2857, 2931. Elemental analysis: Calculated: C 77.74%, H 9.32%. Found: C 77.45%, H 9.60%.

12-TC: ^{1}H NMR ($CDCl_3$, 400M, ppm): δ 7.81 (d, 1H), 7.59-6.83(m, 8H), 6.48 (d, 1H), 5.38 (d, 1H), 4.65 (s, 1H), 4.00 (t, 2H), 2.96-0.68 (m, 70H) FTIR (KBr, cm^{-1}): 520, 824, 1129, 1175, 1250, 1499, 1600, 1730, 2857, 2922. Elemental analysis: Calculated: C 77.98%, H 9.48%. Found: C 78.03%, H 9.58%.

14-TC: ^{1}H NMR ($CDCl_3$, 400M, ppm): δ 7.81 (d, 1H), 7.52-6.92 (m, 8H), 6.48 (d, 1H), 5.38 (d, 1H), 4.65 (s, 1H), 4.00 (t, 2H), 2.87-0.68 (m, 74 H). FTIR (KBr, cm^{-1}):520, 824, 1129, 1175, 1259, 1499, 1600, 1730, 2857, 2931. Elemental analysis: Calculated: C 78.22%, H 9.63%. Found: C 78.11%, H 9.93%.

3. Results and discussion

3.1. Molecular structural characterization

The target compounds m-TC (m = 4, 6, 8, 10, 12 and 14) were synthesized to investigate the influence of the length of terminal chain. Their chemical structures are confirmed by spectroscopic studies. Figure 1 shows the ^{1}H NMR spectra of 10-TC. The related functional groups and protons are noted in the spectra.

^{1}H NMR spectrum of 10-TC revealed that two double peak signals at 7.81 ppm and 6.48 ppm of -CH = CH- group were observed. Resonance signals around 5.37 and 4.67 ppm are usually taken to be confirmatory evidence for the presence of a single hydrogen in cholesterol. A set of multiplets in the range of 7.81 ppm-6.92 ppm confirms

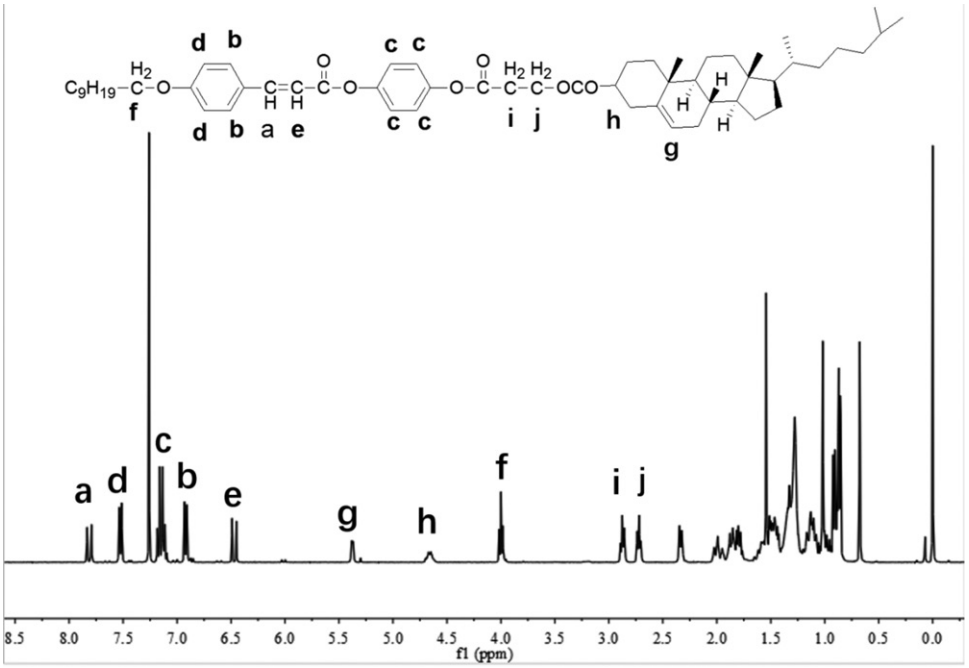

Figure 1. The 400 MHz ^{1}H NMR results of 10-TC in $CDCl_3$.
Note: Below 2.5 ppm is the other 43H (except h and g) in cholesterol moiety and 19 H in the alkyl chain.

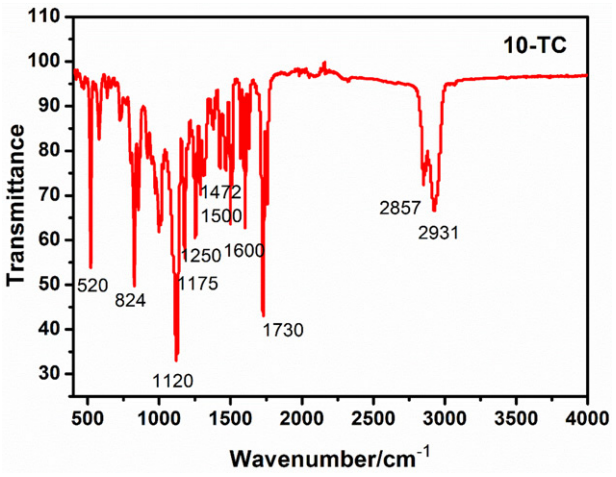

Figure 2. Fourier transform infrared spectrum of target product 10-TC.

the presence of aromatic protons. Methylene is shown by a signal of about 3.94 ppm. Two double peaks of 2.87 ppm and 2.72 ppm, each having two hydrogens, corresponding to hydrogen close to the benzene ring and methylene group. Below 2.5 ppm is the other 43H (except h and g) in cholesterol moiety and 19 H in the alkyl chain. The numbers and chemical shift of hydrogen are in accordance with their molecular structure.

Figure 2 shows the Fourier transform infrared spectrum of 10-TC. The band appearing at 2931 cm^{-1} and 2857 cm^{-1} can be ascribed to stretching of -CH_3 and -CH_2. The

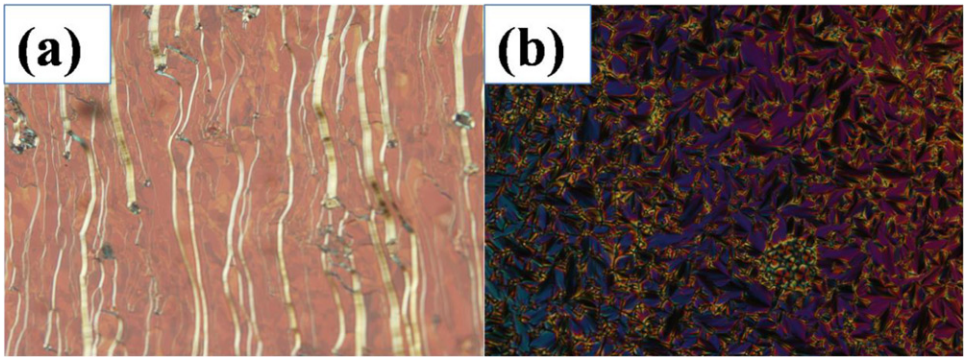

Figure 3. Optical polarizing micrographs of compound 4-TC (a) The oily-streak texture at 155 °C of Ch phase during heating process (b) The focal-conic texture at 187 °C of Ch phase during cooling process.

band appearing at 1730 cm^{-1} can be ascribed to the stretching of the C = O bond belonging to the ester group. The band appearing at 1600 cm^{-1} can be ascribed to stretching of C = C str. vinyl group of cinnamate group of cinnamate. A strong absorption peak appears at 1500 and 1472 cm^{-1}, which is attributed to the C = C stretching vibration of the benzene ring. Formation of the aromatic ether bond (C-O-Ar) was confirmed based on the absorption band at 1250 cm^{-1}.

With the best results of elemental analysis, spectral data obtained by FT-IR and ^{1}H NMR, also confirmed by the only one spot in the TLC (thin layer chromatography), therefore, it is concluded that all target compounds were successfully synthesized.

3.2. Mesomorphic properties

The liquid crystal textures of target compounds m-TC were observed with POM upon heating and cooling cycle.

All the homologues of this series were liquid crystalline; exhibiting mesophase under the POM observation. The optical textures of the LC obtained were observed by POM with a hot stage. The 4-TC exhibited typical cholesteric oily-streak textures when it was heated at 131 °C. By further heating, the birefringence disappeared at 223 °C. During cooling process, a focal-conic cholesteric texture (when sheared, it was changed to oily-streak textures) appeared at 222 °C and the liquid crystalline phase began to crystallize at 39 °C. Figure 3 is a polarized photomicrograph of the product of 4-TC upon heating and cooling process. The LC behavior of 6-TC is very similar to that of 4-TC.

The 8-TC exhibited typical oily-streak textures at 137 °C and a focal-conic texture at 147 °C during heating process. The birefringence disappeared at 236 °C. The 10-TC exhibited typical oily-streak textures at 134 °C and the birefringence disappeared at 204 °C.

In the POM observation of 12-TC, when it was heated at 121 °C, typical SmA* focal-conic texture appeared. By further heating to 154 °C, the liquid crystalline texture was turned to cholesteric oily-streak texture, and the birefringence disappeared at 195 °C. During cooling process, a typical oily-streak textures appeared at 186 °C and the SmA* focal-conic texture appeared at 147 °C, finally the liquid crystalline phase began to

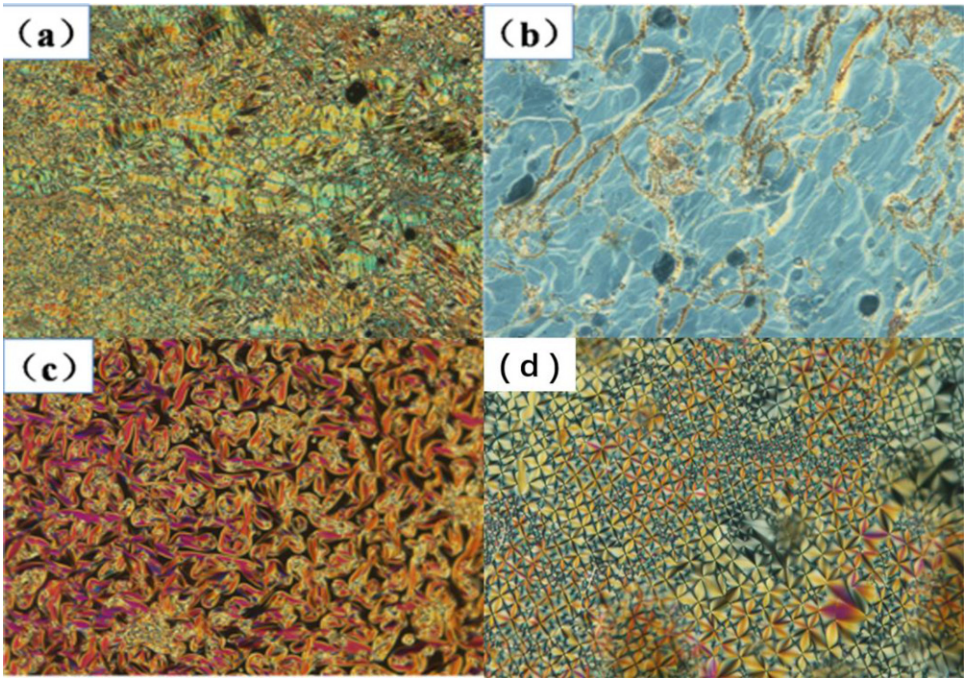

Figure 4. Optical polarizing micrographs of compound 12-TC (a) SmA*, focal-conic texture at 136 °C (b) ChLC, oily-streak texture at 160 °C in heating process (c) ChLC, focal-conic texture at 172 °C (d) SmA*, typical focal-conic texture at 95 °C in cooling process.

crystallize at 89 °C. The LC behavior of 14-TC is very similar to that of 12-TC. The LC behavior of m-TC (8, 10, 12 and 14) is very similar to that of 12-TC during cooling process. The optical texture of the 12-TC is shown in Figure 4.

The phase transition temperatures and corresponding enthalpy changes of compounds were determined using DSC. The DSC traces for target compounds are presented in Figure 5. In the heating process of 4-TC, there are three peaks appeared at 90.2, 130.9 and 222.8 °C. In the cooling processes, two peaks appeared at 222.1°Cand 39.4 °C. Combined with the observations of POM, we can conclude that the corresponding transitions in the heating process are the transition between crystals, the transition from crystal to cholesteric phase and the transition from cholesteric phase to isotropic, respectively. During cooling two peaks appeared, one is the isotropic to cholesteric phase transition at higher temperature, the other is the LC to crystal transition at lower temperature.

The transition process of 6-TC is similar to that of 4-TC. Upon heating 6-TC also exhibits three transitions, in which transitions from crystal to the crystal (82.7 °C), the crystal to cholesteric phase (144.3 °C) and cholesteric phase to isotropic occur (217.2 °C). The transitions in the cooling process are: transition from I to ChLC (216.2 °C), transition from Ch phase to crystal (126.1 °C), and transition between crystals (63.9 °C).

In the DSC curve of 12-TC, four peaks appeared at peak values of 80.5, 120.9, 154.3 and 194.8 °C; accompanying POM observations showed that they represented crystal to crystal transition, melting transition, SmA* to Ch phase transition and cholesteric phase

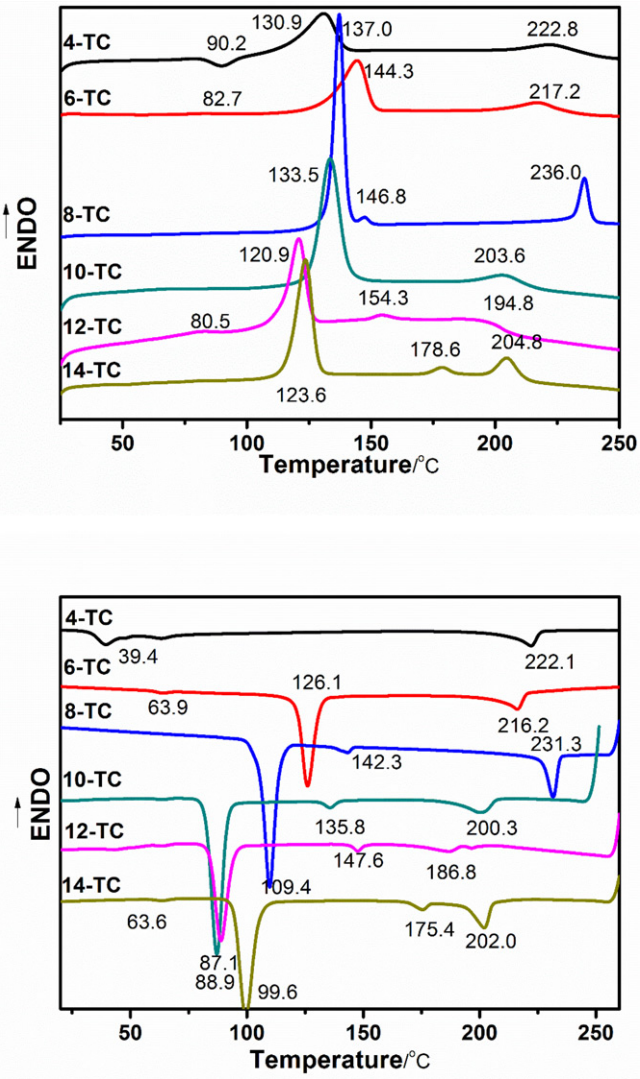

Figure 5. Differential scanning calorimetry traces for m-TC (m= 4, 6, 8, 10, 12 and 14) during heating and cooling.

to isotropic (I), respectively. During cooling three peaks appeared, revealing I to Ch phase transition at higher temperature, Ch to SmA* phase transition, SmA* to crystal transition at lower temperature.

From these two representative analyses, it can be seen that m-TC (m = 4, 6 and 10) mainly undergoes transitions which (transitions between crystals) crystal to cholesteric phases and cholesterol to isotropic transformation during the heating process. The m-TC (m = 8, 12 and 14) mainly undergoes these transitions, which are the transition (transitions between crystals) from crystal to smectic A* phase, the smectic A* phase to the cholesteric phase, and the cholesteric phase to isotropic.

The results determined by the DSC were consistent with that observed under POM.

Table 1. Phase transition temperatures (°C) and associated transition enthalpy values [ΔH, J g^{-1}] from the second heating and first cooling in DSC thermograms (temperature gradient: 10 °C min^{-1}).

Transition temperatures (°C) and associated transition enthalpy values [ΔH, J g^{-1}]									
m	2nd heating								
4	Cr	90.2	Cr	–	–	130.9(18.88)	ChLC	222.8(7.68)	I
6	Cr	82.7	Cr	–	–	144.3(22.08)	ChLC	217.2(6.97)	I
8	–	–	Cr	137.0(8.51)	SmA*	146.8(1.38)	ChLC	236.0(2.61)	I
10	–	–	Cr	–	–	133.5(41.82)	ChLC	203.6(6.99)	I
12	Cr	80.5	Cr	120.9(25.08)	SmA*	154.3(1.33)	ChLC	194.8(4.78)	I
14	–	–	Cr	123.6(30.81)	SmA*	178.6(1.57)	ChLC	204.8(5.97)	I
m	1st cooling								
4	I	222.1(−6.85)	ChLC	–	–	39.4(−8.77)	Cr	–	–
6	I	216.2(−7.48)	ChLC	–	–	126.1(−22.42)	Cr	63.9	Cr
8	I	231.3(−8.17)	ChLC	142.3(−2.06)	SmA*	109.4(−34.63)	Cr	–	–
10	I	200.3(−6.14)	ChLC	135.8(−1.36)	SmA*	87.0(−32.51)	Cr	–	–
12	I	186.8(−1.1)	ChLC	147.6(−2.44)	SmA*	88.9(−22.14)	Cr	–	–
14	I	202.0(−7.30)	ChLC	175.4(−1.31)	SmA*	99.6(−29.51)	Cr	63.6	Cr

Therefore, from combination of the results of DSC studies and POM observation, we also summarize the LC properties of the m-TC (m= 4, 6, 8, 10, 12 and 14) in Table 1. The obtained transition temperatures as a function of carbon numbers (m) are plotted for the aim of clarity and shown in Figure 6. As seen from the data listed in Table 1 and Figure 6, the length of the terminal chains had a considerable influence on the phase types and phase transition temperatures of m-TC. The compounds of m-TC (m = 4, 6, 8, 10, 12 and 14) all have relatively broad cholesteric phases, with the increase of the length of the terminal carbon chain, the phase temperature range gradually decreases. For example, the compound 4-TC is as wide as 91.9 °C, but the compound 14-TC is only 26.2 °C. On the contrary, the temperature range of the smectic phase broadens as the carbon chain increases, and the 14-TC smectic phase temperature range reaches 55 °C. This is mainly due to as the terminal alkyl chain length increases, the aspect ratio of the molecule increases, the polarizability of the molecule decreases, the wide smectic A* phase is easily broadened, and the cholesteric phase is narrowed [46–49]. Lim [50], Selvarasu and Kannan [51] also pointed out that as the length of the alkyl chain at one end increases, the overall polarizability of the molecule increases, which helps to show the smectic texture. In general, the lower alkyl chain liquid crystals are nematic, while the middle chain alkyl chains exhibit nematic and smectic phases. The length of the terminal alkoxy chain affects the melting and clearing temperatures as well as the mesophase ranges. This is because the increase in the length of the terminal alkyl chain makes the force perpendicular to the long axis of the molecule increase.

For compounds of 4-TC and 6-TC, enantiotropic cholesteric phase has emerged, while for those of 8-TC, 10-TC, 12-TC and 14-TC with long terminal chains, smectic A* phase and cholesteric phase were formed. With increasing the number of alkyl in molecules, the smectic A* phase not only appeared but also as m increases the smectic A* phase stability increases as would be anticipated. The changes of this series can be explained in terms of greater molecular length and polarizability of molecule resulting from -C = C- units in the central linkage [51–53].

The result indicates from Figure 6 that the tendency toward smectic A* mesomorphism increases and the temperature of the clearing point decreases, with increasing

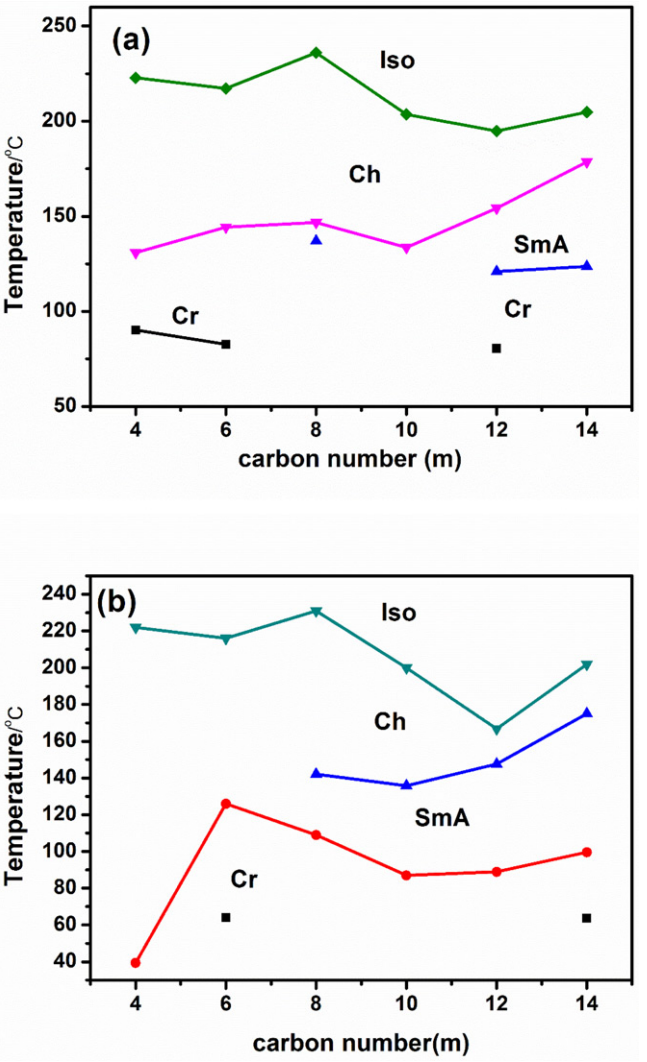

Figure 6. (Colour online) Transition temperature plots as a function of carbon numbers upon heating (a) and cooling (b).

terminal alkoxy chain length. And as the length of the series of terminal alkoxy chains increases, the thermal stability of the smectic A* phase increases. Jin [54–57], Marcelis and Yelamaggad et al [58, 59] have studied the phase behavior of non-symmetric dimers, which contains a flexible alkyl spacer. The type and stability of liquid crystal depend on the length of the terminal alkoxy chain changes. The compounds with shorter end alkoxy chain showed nematic phase while those with longer showed smectic phase.

3.3. Optical properties

The optical properties of cholesteric liquid crystals are attributed to their unusual helical molecular structure and well-defined pitch [60, 61]. When the cholesteric liquid crystals

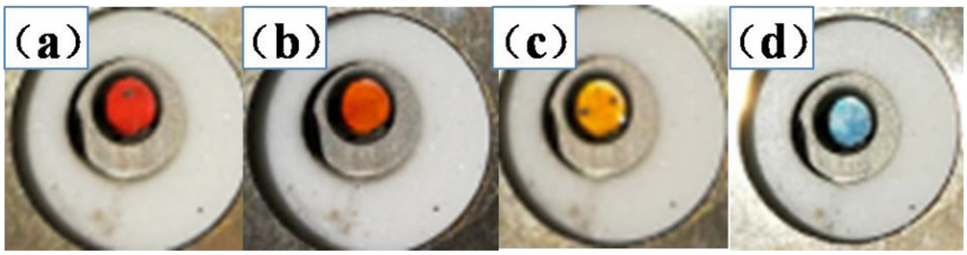

Figure 7. 8-TC shows different colors during heating (a) 170 °C (b) 185 °C (c) 197 °C (d) 231 °C.

are in a uniform parallel orientation, the periodic spiral structure exhibits unique selective reflection optical properties [62–64]. Selective reflection means that the liquid crystal of the cholesteric phase will selectively reflect light of certain wavelengths, thus causing some cholesteric liquid crystals to show brilliant colors under the irradiation of white light. The relationship between the wavelength and the pitch obeys the Bragg equation [65].

To study the change in color, we used a hot stage of a polarizing microscope to observe the color of the sample at different temperatures. All samples disperse the reflected white light and display the rainbow color with temperature increases. The selective reflection wavelengths of cholesteric compounds m-TC decrease with increasing temperature. Figure 7 shows the color change of 8-TC during the heating process. From the figure 7, 8-TC shows the change of four colors with increasing temperature. The reflection color changed from red, orange, yellow to blue with increasing temperature and it was in reverse direction as the temperature decreased in the cooling cycle. This unique optical property is related to the helical molecular structure of cholesteric liquid crystals. As the helical pitch is temperature dependent, the change of temperature will result in the alteration of the pitch of the helical structure of the cholesteric phase. Therefore, the reflection color changes at different temperatures. Yao DS [66], Luo CC [67] and Cha SW [55] synthesize cholesteric liquid crystal compounds and change the pitch by adjusting the temperature to present different colors. The change in temperature causes a change of the pitch of the helical structure of the cholesteric phase. Wang JW [68] has reported a series of new chiral side-chain cholesteric liquid crystalline exhibit different colors at room temperature and the reflection wavelengths change sharply near the temperature of the SmA*-Ch phase transition. When the smectic to the cholesteric phase, the molecules of layer structure are distorted into a cholesteric helix, resulting in the selective reflection wavelength sharply varying [50]. In terms of application, the sharp change of the reflection wavelength near the transition temperature of SmA* phase to the cholesteric phase can be used to determine the distribution of temperature [68–70].

This selective reflection optical characteristic is of great significance in applications such as reflective display technology detection sensors, fiber optics, telecommunications and anti-counterfeiting [71–78].

4. Conclusions

Six liquid crystals compounds m-TC (m = 4, 6, 8, 10, 12 and 14) were prepared and characterized. All the LC phases observed are confirmed by the optical textural

observation and DSC thermogram studies. All of the obtained target compounds displayed very wide mesophase temperature ranges. The effect of terminal alkoxy plays a crucial role in the formation of mesophase. The m-TC (m = 4 and 6) showed cholesteric phase. The m-TC (m = 8, 10, 12, and 14) exhibited the SmA* phase and the cholesteric phase. With increasing the length of terminal alkyl chain in molecules, the aspect ratio of the molecule increases, the polarizability of the molecule decreases, the wide smectic A* phase is easily broadened, and the cholesteric phase is narrowed. The nature of the smectic A* phase formed has been found to depend on the relative length of the terminal chains. In the cholesteric phase, the peak wavelength of the reflected light of all the samples moves toward the short wave direction with increasing temperature, and the reflected white light is dispersed to present a rainbow color. The results of this study provide theoretical and experimental basis for the synthesis and application of liquid crystal compounds with wider mesophase and more stable thermal behavior.

Funding

This research did not receive any specific grant from funding agencies in the public, commercial, or not-for-profit sectors.

References

[1] Tschierske, C., (2013). *Angew. Chem. Int. Ed.*, *52*, 8828.
[2] Park, J. H., Singu, B. S., Choi, O. B. et al. (2017). *Mol. Cryst. Liq. Cryst., 650*, 1.
[3] Fleischmann, E. K., Zentel, R., (2013). *Angew. Chem. Int. Ed.*, *52*, 8810.
[4] Rosu, C., Manaila Maximean D., Kundu, S. et al. (2011). *Electrostatics.*, *69*, 623.
[5] Gilli, J. M., Thiberge, S., Manaila-Maximean, D., (2004), *Mol. Cryst. Liq. Cryst.*, *417*, 207.
[6] Kim, T. H., Lee, C. S., Ramaraj, B. et al. (2008). *Mol. Cryst. Liq. Cryst., 492*, 102.
[7] Kato, T., Yasuda, T., Kamikawa, Y. et al. (2009). *Chem. Commun.*,*40*, 729.
[8] Du, B. G., Hu, J. S., Zhang, B. Y. et al. (2006). *J. Appl. Phys.*, *102*, 5559.
[9] Park, J. H., Choi, O. B., Lee, H. M. et al. (2014). *Mol. Cryst. Liq. Cryst., 599*, 96.
[10] Arakawa, Y., Nakajima, S., Ishige, R. et al. (2012). *J. Mater. Chem.*, *22*, 8394.
[11] Wu. C. C., (2015). *Mol. Cryst. Liq. Cryst., 609*, 31.
[12] Kohout, M., Tuma, J., (2013). *J. Mater. Chem. C.1*, 4962.
[13] He, W. L., Wei, M. J., Yang, H. et al. (2014). *Phys. Chem. Chem. Phys.*, *16*, 5622.
[14] Shanker, G., Yelamaggad, C. V., (2012). *New J. Chem.*, *36*, 918.
[15] Pintre, I. C., Serrano, J. L., Blanca Ros, M., (2010). *J. Mater. Chem.*, *20*, 2965.
[16] He, W. L., Gu, H., Zhao, P. et al. (2017). *Liq. Cryst., 44*, 593.
[17] Tamaoki, N., Moriyama, M., Matsuda. H., (2000). *Angew. Chem. Int. Ed.*, *39*, 509.
[18] Tamaoki. N. (2001). *Adv. Mater.*, *13*, 1135.
[19] Yelamaggad. C. V., (1999). *Mol. Cryst. liq. Cryst., 36*, 149.
[20] Yelamaggad, C. V., Nagamani, S. A., (2001). *Mol. Cryst. liq. Cryst., 363*, 1.
[21] Craig, A. A., Imrie, C. T., (1994). *J. Mater. Chem.*, *4*, 1705.
[22] Luo, C. C., Jia, Y. G., Song, K. M. et al. (2017). *Liq. Cryst., 44*, 1.
[23] Mocanu, A. S., Ilis, M., Dumitrascu, F. et al. (2010). *Inorg. Chim. Acta.*, *363*, 729.
[24] Imrie, C. T., Henderson, P. A., (2002). *Curr. Opin. Colloid In.*, *7*, 298.
[25] So, B. K., Jang, M. C., Park, J. H. et al. (2002). *Opt. Mater., 21*, 685.
[26] Praveen, P. L., Ojha, D. P., (2014). *J. Mol. Liq.*, *197*, 106.
[27] Varghese, N., Shetye, G. S., Yang, S. et al. (2013). *J. Colloid Interface Sci.*, *412*, 95.
[28] So, B. K., Kim, Y. S., Choi, M. M. et al. (2004). *Liq. Cryst.*, *31*, 169.
[29] Craig, A. A., Imrie. C. T., (1995). *Macromolecules.*, *28*, 3617.

[30] Yeap, G. Y., Balamurugan, S., Srinivasan, M. V. et al. (2013). *New. J. Chem*., *37*, 1906.
[31] Yeap. G. Y., (2009). *Mol. Cryst. Liq. Cryst., 506*, 56.
[32] Wu. C. C., (2007). *Mater. Lett*., *61*, 1380.
[33] Weissflog, W., adasi, H. N., Dunemann, U. et al. (2001). *J. Mater. Chem*., *11*, 2748.
[34] Morale, F., Date, R. W., Guillon, D. et al. (2003). *Chem. Eur. J*., *9*, 2484.
[35] Blatch, A. E., Luckhurst. G. R., (2000). *Liq. Cryst*., *27*, 775.
[36] Shen, D., Pegenau, A., Diele, S. et al. (2000). *J. Am. Chem. Soc*., *122*, 1593.
[37] Attard, G. S., Date, R. W., Imrie, C. T. et al. (2006). *Liq. Cryst*., *16*, 529.
[38] Mohammad, A. T., Yeap, G. Y., Osman H., (2014). *Turk. J. Chem*., *38*, 443.
[39] Pathak, S. K., Nath, S., De, J. et al. (2017). *New J. Chem*., *41*, 4680.
[40] Hu, J. S., He, X. Z., Cheng. C. Z., (2004). *Liq. Cryst*., *31*, 1357.
[41] Wu. C. C. (2007). *Liq. Cryst., 34*, 283.
[42] Yelamaggad, C. V., Prabhu, R., Shanker, G. et al. (2009). *Liq. Cryst*., *36*, 247.
[43] Yelamaggad, C. V., Shashikala, I. S., Liao, G. et al. (2006). *Chem. Mater*., *18*, 6100.
[44] Yelamaggad. C. V., Shanker. G. (2017). *Liq. Cryst*., *34*, 1045.
[45] Ma, S., Cai, Y., Tu, Y. et al. (2016). *Polym. Chem*., *7*, 3520.
[46] Yelamaggad, C. V., Nagamani, S. A., Hiremath, U. S. et al. (2001). *Liq. Cryst*., *28*, 1009.
[47] Weissflog, W., Dunemann, U., Schroder, M. W., (2005). *J. Mater. Chem*., *15*, 939.
[48] Niori, T., Adachi, S., Watanabe, J., (1995). *Liq. Cryst*., *19*, 139.
[49] Henderson, P. A., Seddon, J. M., Imrie, C. T., (2005). *Liq. Cryst*., *32*, 1499.
[50] Lim, Y. W. C., Ha, S. T., Yeap, G. Y., (2017). *J. Taibah Univer Sci*., *11*, 133.
[51] Selvarasu, C., Kannan, P., (2016). *J. Mol. Struct*., *1125*, 234.
[52] Hsieh, C. J., Hsu, C. S., Hsiue, G. H. et al. (1990). *Mater. Chem. Phys., 28*, 425.
[53] Luo, C. C., Jia, Y. G., Sun, B. F. et al. (2017). *New J. Chem*., *41*, 3677.
[54] Hardouin, F., Achard, M. F., Laguerre, M., Jin, J. I., (1999). *Liq. Cryst*., *26*, 589.
[55] Cha, S. W., Jin, J. I., Laguerre, M. et al. (1999). *Liq. Cryst*., *26*, 1325.
[56] Lee, D. W., Jin, J. I., Laguerre, M. et al. (2000). *Liq. Cryst*., *27*, 145.
[57] Cha, S. W., Jin, J. I., Achard, M. F., (2002). *Liq. Cryst*., *29*, 755.
[58] Marcelis, A. T. M., Koudijs, A., Klop, E. A. et al. (2001). *Liq. Cryst*., *28*, 881.
[59] Yelamaggad, C. V., Anithanagamani, S., Hiremath, U. S. et al. (2002). *Liq. Cryst*., *29*, 1401.
[60] Dewitte, P. V., Carlosgalan. J., (1998). *Liq. Cryst., 24*, 819.
[61] Wu, X. J., Cao, H., Guo, R. W. et al. (2013). *Polym. Adv. Tech*., *24*, 228.
[62] Huang, Y. M., Guo, Y. T., Ma, Q. L. et al. (2010). *Key. Eng. Mater*., *428*, 94.
[63] Mathew George, Ajay Mallia, V., Sudhadevi Antharjanam, P. K. et al. (2000). *Mol. Cryst. Liq. Cryst*., *350*, 125.
[64] Kurihara, S., Kanda, T., Nagase, T. et al. (1998). *Appl. Phys. Lett*., *73*, 2081.
[65] Gvozdovskyy. I., (2015). *Liq. Cryst*., *42*, 1391.
[66] Yao, D. S., Zhang, B. Y., Zhang, W. W. et al. (2008). *J. Mol. Struct., 881*, 83.
[67] Luo, C. C., Jia, Y. G., Song, K. M. et al. (2017). *Liq. Cryst*., **44**, 2366.
[68] So, B. K., Kim, H. J., Lee, S. M., et al. (2006). *Dyes Pigments*., *70*, 38.
[69] Wang, J. W., Zhang. B. Y., (2003). *Colloid Polym Sci*., *291*, 2917.
[70] Natarajan, L. V., Wofford, J. M., Tondiglia, V. P. et al. (2008). *J. Appl. Phys*., *103*, 263.
[71] Hu, J. S., Zhang, B. Y., Pan, W. et al. (2004). *Poly. J*., *36*, 920.
[72] Heppke, G., Parghi, D. D., Sawade, H., (2000). *Liq. Cryst*., *27*, 313.
[73] Hu, J. S., Zhang, B. Y. et al. (2003). *Macromolecules., 36*, 2849.
[74] Hu, J. S., Zhang, B. Y. Yao, D. et al. (2004). *Liq. Cryst*., *31*, 393.
[75] Hiremath, U. S., Sonar, G. M., Shankar Rao, D. S. et al. (2011). *J. Mater. Chem*., *21*, 4064.
[76] Hu, J. S., Wei, K. Q., Zhang, B. Y. et al. (2008). *Liq. Cryst., 35*, 925.
[77] Shanker, G., Yelamaggad. C. V., (2011). *J. Phys. Chem. B*., *115*, 10849.
[78] Yilmaz. S., (2008). *Mater. Chem. Phys*., *110*, 140.